

AD-A214 979

DTIC FILE COPY

①

REPORT DOCUMENTATION PAGE			Form Approved OMB No. 0704-0188	
<small>Public reporting burden for this collection of information is estimated to average 1 hour per response, including the time for reviewing instructions, searching existing data sources, gathering and maintaining the data needed, and completing and reviewing the collection of information. Send comments regarding this burden estimate or any other aspect of this collection of information, including suggestions for reducing this burden, to Washington Headquarters Services, Directorate for Information Operations and Reports, 1215 Jefferson Davis Highway, Suite 1204, Arlington, VA 22202-4302, and to the Office of Management and Budget, Paperwork Reduction Project (0704-0188), Washington, DC 20503.</small>				
1. AGENCY USE ONLY (Leave blank)	2. REPORT DATE June 1983	3. REPORT TYPE AND DATES COVERED Final (30 June 81-30 Sep 82)		
4. TITLE AND SUBTITLE HYBRID FINITE ELEMENT ANALYSIS OF FREE EDGE EFFECT IN SYMMETRIC COMPOSITE LAMINATES		5. FUNDING NUMBERS 61102F 2307/B2		
6. AUTHOR(S) S.W. Lee J.J. Rhiu S.C. Wong		7. PERFORMING ORGANIZATION NAME(S) AND ADDRESS(ES) University of Maryland Department of Aerospace Engineering College Park, MD 20742		
8. PERFORMING ORGANIZATION REPORT NUMBER AFOSR-TR-89-1607		9. SPONSORING/MONITORING AGENCY NAME(S) AND ADDRESS(ES) AFOSR BLDG 410 BAF3 DC 20332-6448		
10. SPONSORING/MONITORING AGENCY REPORT NUMBER AFOSR-81-0203		11. SUPPLEMENTARY NOTES		
12a. DISTRIBUTION/AVAILABILITY STATEMENT Approved for public release; distribution unlimited.		12b. DISTRIBUTION CODE		
13. ABSTRACT (Maximum 200 words) <div style="text-align: center;"> <p>DTIC ELECTE DECO 6 1989 S B D</p> </div>				
14. SUBJECT TERMS		15. NUMBER OF PAGES 61		
		16. PRICE CODE		
17. SECURITY CLASSIFICATION OF REPORT unclassified	18. SECURITY CLASSIFICATION OF THIS PAGE unclassified	19. SECURITY CLASSIFICATION OF ABSTRACT	20. LIMITATION OF ABSTRACT	

NSN 7540-01-280-5500

Standard Form 298 (890104 Draft)
Prescribed by ANSI Std. Z39-18
298-104

89 12 05 123

AFOSR TR

HYBRID FINITE ELEMENT ANALYSIS OF FREE EDGE
EFFECT IN SYMMETRIC COMPOSITE LAMINATES

S. W. Lee
J. J. Rhiu
S. C. Wong

Department of Aerospace Engineering
University of Maryland
College Park, Maryland 20742

June 1983

PREPARED FOR
Air Force Office of Scientific Research
United States Air Force

UNDER
Grant No. AFOSR-81-0203

APPROVED FOR PUBLIC RELEASE; DISTRIBUTION UNLIMITED.

ACKNOWLEDGEMENT

This research task was supported by the U.S. Air Force Office of Scientific Research (Grant No. AFOSR-81-0203) with Dr. Anthony K. Amos as the program monitor.

The work was conducted by the Department of Aerospace Engineering, University of Maryland, College Park, Maryland.

The bulk of computing time was provided by the Computer Science Center at the University of Maryland.



Accession For	
NTIS GRA&I	<input checked="checked" type="checkbox"/>
DTIC TAB	<input type="checkbox"/>
Unannounced	<input type="checkbox"/>
Justification	
By	
Distribution/	
Availability Codes	
Dist	Avail and/or Special
A-1	

TABLE OF CONTENTS

<u>Section</u>	<u>Page</u>
1. INTRODUCTION	1
2. FORMULATION	3
2.1 Problem Description	3
2.2 Hybrid Finite Element Formulation	4
3. NUMERICAL EXAMPLES	16
4. CONCLUSION	19
REFERENCES	20
FIGURES	23
APPENDIX	34
A.1 Anisotropic Elasticity with Prescribed Uniform Uniaxial Strain	34
A.2 Constant Stress Field	40
A.3 Assumed Stress Field (Singular and Nonsingular)	45

1. INTRODUCTION

The analytical study of the nature of interlaminar stresses near stress-free edges has been the subject of substantial research interest. Such studies are significant because the high interlaminar stresses or stress singularities near stress-free edges may cause delamination failure as shown by experimental investigations [1-3]. Also the accurate prediction of these stresses may be useful in the design of test specimens for investigation of laminate strength [4]. One of the first analytical studies on interlaminar stresses near stress-free edges was published by Pipes and Pagano [5]. In their study, finite difference technique was applied to a symmetric finite-width composite laminate subjected to uniform uniaxial strain. Subsequently other techniques were used to solve similar problems. Among these are the boundary layer or the perturbation method [6-8], Galerkin method [9] and the finite element method [10-13]. However, in these studies the exact nature of stress singularities at the free edges were not taken into account in the formulation. Therefore, perhaps except for Reference 13, the accuracy of solutions near the free-edge interface appears marginal at best. In the finite element analysis reported in Reference 13, extremely fine meshes were used near the free-edge interface, resulting in a finite element model with a large number of degrees of freedom. Recently the exact nature of stress singularities near the free-edge interfaces in cross ply and angle ply composites has been investigated [14-18]. Reference 18 also includes interlaminar stress distribution determined by the boundary collocation method.

In this report, we present an efficient hybrid finite element method for analysis of interlaminar stress or free edge effect in symmetric

composite laminates subject to uniform uniaxial strain. Both cross ply and angle ply laminates are considered. The main feature of the present study is the use of a special hybrid element with an embedded stress singularity. The effectiveness of the hybrid finite element method, when applied to problems with a singularity, such as a crack, has been amply demonstrated by Pian and other people [19-21]. Especially the bi-material crack analysis by Lin and Mar [22] is quite relevant to the present interlaminar stress analysis.

In the next section, a formulation for both special and regular hybrid elements are given. Numerical examples are treated in the third section. A detailed discussion on the determination of assumed stress and displacement field is included in the Appendix.

2. FORMULATION

2.1 Problem Description

Figure 1 shows a long, symmetric cross ply or angle ply composite laminate loaded in the z direction. The laminate has four plies, each with thickness h . The width of the laminate is $2b$. For the region away from the ends, the laminate can be considered to be subject to uniform uniaxial strain $\epsilon_{zz} = \epsilon_0$ [5,23], and the displacement u , v and w in x , y and z directions respectively can be written as

$$\begin{aligned}u &= U(x,y) \\v &= V(x,y) \\w &= \epsilon_0 z + W(x,y)\end{aligned}\tag{1}$$

where U , V , W are functions independent of z . For cross ply laminates $W(x,y) = 0$. Also stress is independent of z , and thus equilibrium eqs. are:

$$\begin{aligned}\frac{\partial \sigma_{xx}}{\partial x} + \frac{\partial \sigma_{xy}}{\partial y} &= 0 \\ \frac{\partial \sigma_{xy}}{\partial x} + \frac{\partial \sigma_{yy}}{\partial y} &= 0 \\ \frac{\partial \sigma_{xz}}{\partial x} + \frac{\partial \sigma_{yz}}{\partial y} &= 0\end{aligned}\tag{2}$$

Thus the problem reduces essentially to a two-dimensional boundary value problem in x,y plane. For cross ply laminates $\sigma_{xz} = \sigma_{yz} = 0$.

2.2 Hybrid Finite Element Formulation

In hybrid finite element approximation, a cross section of the laminate normal to the z coordinate is divided into two regions, (see fig. 2). The cross-hatched region in fig. 2 contains both the ply interface and the stress-free edge. Since stress singularity is present at the junction of the ply interface and the stress-free edge, this region is modeled by a single special hybrid element with proper stress singularity terms. The rest of the plane is modeled with many ordinary hybrid elements.

For actual formulation of hybrid finite elements, we may start from the Hellinger-Reissner principle or the modified complementary energy principle [24-25]. Both are two-field variational principle with displacement and stress components as independent variables.

For the Hellinger-Reissner principle, the functional π_R is expressed as follows:

$$\pi_R = \int_V \sigma_{ij} \bar{\epsilon}_{ij} dV - \int_V \frac{1}{2} S_{ijkl} \sigma_{ij} \sigma_{kl} dV - \int_{S_\sigma} \bar{T}_i \bar{u}_i dS \quad (3)$$

where

σ_{ij} = stress tensor

$\bar{\epsilon}_{ij} = \frac{1}{2} (u_{i,j} + u_{j,i})$ = strain tensor in terms of displacement vector

\bar{u}_i = displacement vector

S_{ijkl} = compliance tensor

\bar{T}_i = applied traction vector

V = volume of the solid body

S_σ = portion of the surface where traction is applied

The stationarity of π_R leads to

$$\delta\pi_R = \int_V \sigma_{ij} \delta\bar{\epsilon}_{ij} dV + \int_V (\bar{\epsilon}_{ij} - \epsilon_{ij}) \delta\sigma_{ij} dV - \int_{S_\sigma} \bar{T}_i \delta\bar{u}_i dS = 0 \quad (4)$$

where

$$\delta\bar{\epsilon}_{ij} = \frac{1}{2} (\delta u_{i,j} + \delta u_{j,i}) \quad (5)$$

In eq. (4), $\delta\bar{\epsilon}_{ij}$ and $\delta\sigma_{ij}$ can be interpreted as virtual strain tensor and virtual stress tensor respectively. For the problem to be considered here, the traction vector $\bar{T}_i = 0$. Now if V_1 represents the volume of the special element and V_2 the rest, then $\delta\pi_R = 0$ can be expressed as

$$\delta\pi_R = \delta\pi_{R_1} + \delta\pi_{R_2} = 0 \quad (6)$$

where

$$\delta\pi_{R_k} = \int_{V_k} \sigma_{ij} \delta\bar{\epsilon}_{ij} dV + \int_{V_k} (\bar{\epsilon}_{ij} - \epsilon_{ij}) \delta\sigma_{ij} dV \quad (k=1,2) \quad (7)$$

(A) Regular Element

The region away from the free-edge ply interface is modeled by regular hybrid stress elements since no singularity is expected there. The finite element modeling is accomplished by using the expression for $\delta\pi_{R_2}$ in eq. (7). For the problem considered here, the volume integral in eq. (7) reduces to an integral over area A_2 . Written in matrix form,

$$\delta\pi_{R_2} = \int_{A_2} \delta\bar{\epsilon}^T \underline{\sigma} dA + \int_{A_2} \delta\sigma^T (\bar{\epsilon} - \epsilon) dA \quad (8)$$

The superscript T represents the transpose.

Since $\epsilon_{zz} = \bar{\epsilon}_{zz} = \epsilon_0$ is given, the strain vector $\underline{\epsilon}$ and the stress vector $\underline{\sigma}$ are expressed in component form as follows:

$$\underline{\epsilon} = \begin{Bmatrix} \bar{\epsilon}_{xx} \\ \bar{\epsilon}_{yy} \\ \bar{\epsilon}_{yz} \\ \bar{\epsilon}_{zx} \\ \bar{\epsilon}_{xy} \end{Bmatrix} \quad (9)$$

$$\underline{\sigma} = \begin{Bmatrix} \sigma_{xx} \\ \sigma_{yy} \\ \sigma_{yz} \\ \sigma_{zx} \\ \sigma_{xy} \end{Bmatrix} \quad (10)$$

For cross ply laminates, $\bar{\epsilon}_{yz} = \bar{\epsilon}_{zx} = \sigma_{yz} = \sigma_{zx} = 0$. Similar expressions hold true for $\delta\underline{\epsilon}$ and $\delta\underline{\sigma}$. Strain vector $\underline{\epsilon}$ is related to stress vector $\underline{\sigma}$ through the following eq.

$$\underline{\epsilon} = \underline{B} \underline{\sigma} + \underline{\epsilon}_0 \quad (11)$$

where \underline{B} is now a modified compliance matrix, and $\underline{\epsilon}_0$ plays the role of an initial strain vector. See Appendix A.1 for derivation of \underline{B} and $\underline{\epsilon}_0$. Substituting eq. (11) into eq. (8)

$$\delta\pi_{R_2} = \int_{A_2} \delta\underline{\epsilon}^T \underline{\sigma} dA + \int_{A_2} \delta\underline{\sigma}^T (\underline{\epsilon} - \underline{B} \underline{\sigma} - \underline{\epsilon}_0) dA \quad (12)$$

For finite element approximation, the displacement vector \underline{u} is assumed in each element as

$$\underline{\bar{u}} = \underline{N} \underline{q}_e \quad (13)$$

where

\underline{N} = shape function matrix

\underline{q}_e = element nodal displacement vector

Then symbolically

$$\underline{\bar{\epsilon}} = \underline{\bar{B}} \underline{q}_e \quad (14)$$

and also

$$\delta \underline{\bar{\epsilon}} = \underline{\bar{B}} \delta \underline{q}_e \quad (15)$$

The assumed stress field satisfies equilibrium in each element, and can be expressed as

$$\underline{\sigma} = \underline{P} \underline{\beta} \quad (16)$$

where

\underline{P} = stress shape function matrix

$\underline{\beta}$ = the vector of unknown stress parameters

Also,

$$\delta \underline{\sigma} = \underline{P} \delta \underline{\beta} \quad (17)$$

Substituting eqs. (13) - (17) into eq. (12)

$$\delta \pi_{R_2} = \sum [\delta \underline{q}_e^T \underline{G}^T \underline{\beta} + \delta \underline{\beta}^T (\underline{G} \underline{q}_e - \underline{H} \underline{\beta} - \underline{G}_0)] \quad (18)$$

where

$$\begin{aligned}\underline{G} &= \int \underline{P}^T \underline{B} \, dA \\ \underline{H} &= \int \underline{P}^T \underline{B} \underline{P} \, dA \\ \underline{G}_0 &= \int \underline{P}^T \underline{\epsilon}_0 \, dA\end{aligned}\tag{19}$$

The Σ notation indicates summation over all regular elements. From eq. (18),

$$\underline{G} \, \underline{q}_e - \underline{H} \, \underline{\beta} - \underline{G}_0 = 0\tag{20}$$

for arbitrary $\delta \underline{\beta}$. From eq. (20)

$$\underline{\beta} = \underline{H}^{-1} (\underline{G} \, \underline{q}_e - \underline{G}_0)\tag{21}$$

Substituting eq. (21) into eq. (18)

$$\begin{aligned}\delta \pi_{R_2} &= \Sigma \, \delta \underline{q}_e^T \, \underline{G}^T \, \underline{H}^{-1} (\underline{G} \, \underline{q}_e - \underline{G}_0) \\ &= \Sigma \, \delta \underline{q}_e^T (\underline{k}_e \, \underline{q}_e - \underline{Q}_e)\end{aligned}\tag{22}$$

where

$$\underline{k}_e = \underline{G}^T \, \underline{H}^{-1} \, \underline{G}\tag{23}$$

is the element stiffness matrix and

$$\underline{Q}_e = \underline{G}^T \, \underline{H}^{-1} \, \underline{G}_0\tag{24}$$

is the element nodal load vector due to prescribed strain ϵ_0 .

The regular elements in the present study are four node element with isoparametric representation for the assumed displacement field. The assumed stress field is linear and satisfies equilibrium equation within each element. Thus for the cross ply cases, a regular element has eight nodal degrees of freedom and the following stress field with seven stress parameters:

$$\begin{aligned}\sigma_{xx} &= \beta_1 + \beta_2 x + \beta_3 y \\ \sigma_{yy} &= \beta_4 + \beta_5 x + \beta_6 y \\ \sigma_{xy} &= \beta_7 - \beta_6 x - \beta_2 y\end{aligned}\tag{25}$$

For angle ply case, an element has twelve nodal degrees of freedom. For the assumed stress field, the following σ_{xz} and σ_{yz} components are added to those in eq. (25)

$$\begin{aligned}\sigma_{xz} &= \beta_8 + \beta_9 x + \beta_{10} y \\ \sigma_{yz} &= \beta_{11} + \beta_{12} x - \beta_9 y\end{aligned}\tag{26}$$

(B) Special Element

The special element incorporates stress singularity. In addition, the stress-free condition along the edge and the bonding condition along the ply interface are exactly satisfied, (See fig. 4.).

Using the divergence theorem, $\delta\pi_{R_1}$ in eq. (7) can be transformed to

$$\delta\pi_{R_1} = \int_{S_1} T_i \delta\bar{u}_i + \int_{S_1} \delta T_i (\bar{u}_i - u_i) dS \quad (27)$$

for stress which is in equilibrium and also compatible. In eq. (27) u_i is the displacement integrated from stress and is independent of \bar{u}_i . Written in matrix form,

$$\delta\pi_{R_1} = \int_{S_1} \delta\bar{\mathbf{u}}^T \mathbf{T} dS + \int_{S_1} \delta\mathbf{T}^T (\bar{\mathbf{u}} - \mathbf{u}) dS \quad (28)$$

Since

$$\mathbf{u} = \begin{Bmatrix} u \\ v \\ w \end{Bmatrix} = \begin{Bmatrix} U(x,y) \\ V(x,y) \\ \epsilon_0 z + W(x,y) \end{Bmatrix} \quad (29a)$$

and

$$\bar{\mathbf{u}} = \begin{Bmatrix} \bar{u} \\ \bar{v} \\ \bar{w} \end{Bmatrix} = \begin{Bmatrix} \bar{U}(x,y) \\ \bar{V}(x,y) \\ \epsilon_0 z + \bar{W}(x,y) \end{Bmatrix} \quad (29b)$$

$\delta\pi_{R_1}$ can be rewritten as

$$\delta\pi_{R_1} = \int_{S_1} \delta\bar{\mathbf{u}}^T \mathbf{T} dS + \int_{S_1} \delta\mathbf{T}^T (\bar{\mathbf{u}} - \mathbf{u}) dS \quad (30)$$

where

$$\underline{U} = \begin{Bmatrix} \bar{U} \\ \bar{V} \\ \bar{W} \end{Bmatrix} \quad (31)$$

and

$$\underline{T} = \begin{Bmatrix} T_x \\ T_y \\ T_z \end{Bmatrix} = \begin{bmatrix} \sigma_{xx} & \sigma_{xy} & \sigma_{xz} \\ \sigma_{xy} & \sigma_{yy} & \sigma_{yz} \\ \sigma_{xz} & \sigma_{yz} & \sigma_{zz} \end{bmatrix} \begin{Bmatrix} l \\ m \\ n \end{Bmatrix} \quad (32)$$

In eq. (32), l , m and n are the components of a unit vector normal to the surface. Similar expressions hold for U , $\delta \underline{U}$ and $\delta \underline{T}$. In eq. (28), integration is defined over the surface. However, for the present problem, it reduces to a line integral along the element boundary.

For finite element approximation, it is convenient to separate $\underline{\sigma}$ and \underline{U} such that

$$\begin{aligned} \underline{\sigma} &= * \underline{\sigma} + {}^0 \underline{\sigma} \\ \underline{U} &= * \underline{U} + {}^0 \underline{U} \end{aligned} \quad (33)$$

Here ${}^0 \underline{\sigma}$ term is constant stress predetermined to take care of the ϵ_0 term in eq. (11). The $* \underline{\sigma}$ terms represent the assumed stress and are free of ϵ_0 terms. The ${}^0 \underline{U}$ and $* \underline{U}$ vectors correspond to ${}^0 \underline{\sigma}$ and $* \underline{\sigma}$ respectively. The pair ${}^0 \underline{U}$ and ${}^0 \underline{\sigma}$ satisfies equilibrium, compatibility and stress-free conditions along the edge as well as the bonding condition along the ply interface. See Appendix A.2 for details. The pair $* \underline{U}$ and

σ^* also satisfies all these conditions.

Symbolically, the assumed stress σ^* can be expressed as

$$\sigma^* = P \beta \quad (34)$$

where β is the vector of unknown parameters. The σ^* vector includes singular as well as regular stress terms. From eqs. (32) and (33), we may write

$$\underline{\tau} = \sigma^* \underline{\tau} + {}^0 \underline{\tau} \quad (35)$$

And then, from eq. (32) and (34), $\sigma^* \underline{\tau}$ may be written symbolically as

$$\sigma^* \underline{\tau} = R \beta \quad (36)$$

The $\sigma^* \underline{u}$ vector is also expressed symbolically as

$$\sigma^* \underline{u} = L \beta \quad (37)$$

The displacement vector \underline{u} is assumed in terms of element nodal displacement vector q_e such that

$$\underline{u} = N q_e \quad (38)$$

The N matrix now represents the shape function matrix along the element boundary.

With eqs. (36) to (38), $\delta \pi_{R_1}$ in eq. (28) can be written as

$$\delta \pi_{R_1} = \delta q_e^T \underline{G}^T \beta + \delta q_e^T Q_0 + \delta \beta^T (\underline{G} q_e - H \beta - G_0) \quad (39)$$

where

$$\underline{G} = \int_{S_1} \underline{R}^T \underline{N} dS$$

$$\underline{H} = \int_{S_1} \underline{R}^T \underline{L} dS$$

(40)

$$\underline{Q}_0 = \int_{S_1} \underline{R}^T {}^0\underline{I} dS$$

$$\underline{G}_0 = \int_{S_1} \underline{R}^T {}^0\underline{U} dS$$

The \underline{H} matrix is symmetric although the integrand $\underline{R}^T \underline{L}$ is not. It should be noted that the path of line integral in eq. (40) does not include the stress-free edge and the ply interface. Thus the integration path does not cross the singular point. In fact, this is the essence of hybrid formulation for analysis of cracked solids [19]. From eq. (39)

$$\underline{G} \underline{q}_e - \underline{H} \underline{\beta} - \underline{G}_0 = 0$$

or

$$\underline{\beta} = \underline{H}^{-1} (\underline{G} \underline{q}_e - \underline{G}_0) \quad (41)$$

Substituting eq. (41) into eq. (39),

$$\begin{aligned} \delta \pi_{R_1} &= \delta \underline{q}_e^T \underline{G}^T \underline{H}^{-1} (\underline{G} \underline{q}_e - \underline{G}_0) + \delta \underline{q}_e^T \underline{Q}_0 \\ &= \delta \underline{q}_e^T (\underline{k}_e \underline{q}_e - \underline{Q}_e) \end{aligned} \quad (42)$$

where

$$\underline{k}_e = \underline{G}^T \underline{H}^{-1} \underline{G} \quad (43)$$

is the stiffness matrix of the special element and

$$\underline{Q}_e = \underline{G}^T \underline{H}^{-1} \underline{G}_0 - \underline{Q}_0 \quad (44)$$

is the element load vector.

The special element used in the present study has nine nodes as shown in Fig. 3. The displacement between two nodes is linear and thus compatible with the adjacent regular elements. The number of unknown parameters in the $\underline{\beta}$ vector is three for cross ply case and four for angle ply case. See Appendix A.3 for details on the assumed stress field.

(C) Summing or Assembling

The finite element equation for the whole problem is derived by summing $\delta\pi_{R_1}$ and $\delta\pi_{R_2}$ such that

$$\delta\pi_R = \sum \delta q_e^T (\underline{k}_e \underline{q}_e - \underline{Q}_e) = \delta q (\underline{k} \underline{q} - \underline{Q}) = 0 \quad (45)$$

Now the summation notation stands for summing or assembling over all elements and

\underline{q} = global nodal displacement vector

\underline{k} = global stiffness matrix

\underline{Q} = global load vector

For arbitrary δq , we obtain

$$\underline{k} \underline{q} = \underline{Q} \tag{46}$$

which can be solved for \underline{q} .

3. NUMERICAL EXAMPLES

The effectiveness of the present method has been tested by solving three examples of four-ply laminates. They are $[90^\circ/0^\circ]_s$ and $[0^\circ/90^\circ]_s$ cross ply laminates and a $[\pm 45^\circ]_s$ angle ply laminate as shown in fig. 5. The geometrical dimensions and material properties used in the present study are given as follows:

(a) geometry

half width $b = 24"$

ply thickness $h = 3"$

(b) material property

$$E_{11} = 20.0 \times 10^6 \text{ psi}$$

$$E_{22} = 2.1 \times 10^6 \text{ psi}$$

$$\nu_{12} = \nu_{23} = \nu_{31} = 0.21$$

$$G_{12} = G_{23} = G_{31} = 0.85 \times 10^6 \text{ psi}$$

These properties are the same as those used by other people [5,9,12]. Due to symmetry, only a quarter of the section (the upper left part) was modeled. Two different meshes, coarse and fine, were used to check convergence. Figure 6 shows these meshes in scale. The number of nodes for the coarse and fine meshes are 111 and 159 respectively.

(A) Cross Ply Case

Figures 7 and 8 shows stress distribution along the 90° - 0° ply interface at $y = h$ for both $[90^\circ/0^\circ]_s$ and $[0^\circ/90^\circ]_s$ laminates. These results are for the fine mesh. Although they are not shown, solutions

obtained by the coarse mesh are very close to those by the fine mesh, indicating convergence. Note that for convenience a new coordinate \bar{x} is introduced as shown in fig. 2. The \bar{x} coordinate is introduced such that $\bar{x} = 0$ at the free edge and $\bar{x} = b$ at the center.

Another measure of convergence is to check the value of free parameter β_1 corresponding to the singular stress term. For the $[90^\circ/0^\circ]_s$ laminate, the computed values of β_1 are $0.1044 \times 10^8 \epsilon_0$ for the coarse mesh and $0.1036 \times 10^8 \epsilon_0$ for the fine mesh. For the $[0^\circ/90^\circ]_s$ laminate, these values are $-0.4384 \times 10^6 \epsilon_0$ for the coarse mesh and $-0.4338 \times 10^6 \epsilon_0$ for the fine mesh.

In fig. 7, normal stress σ_{yy} shows high gradient near the free edge for both $[0^\circ/90^\circ]_s$ and $[90^\circ/0^\circ]_s$ laminates. The $[90^\circ/0^\circ]_s$ case is particularly interesting. Results reported by Wang and Crossman [9] and Spilker [12] indicates very small σ_{yy} at the free edge. On the other hand, the present result shows ever-increasing high positive normal stress confined to extremely narrow region at the edge. This result is in agreement with that by Raju [13], and clearly indicates existence of stress singularity. It appears that, although Wang and Crossman, and Spilker used very fine meshes near the edge, the size of elements was not small enough to capture the detailed picture. Meanwhile the size of elements used in reference 13 at the edge was extremely small, resulting in a model with an excessively large number of unknowns. Figure 8 shows σ_{xy} distribution. It attains maximum value very close to the free edge. Of course it drops to zero at the free edge itself.

(B) $[\pm 45^\circ]_s$ Angle Ply Case

In this example, computed values of β_1 are $0.1131 \times 10^8 \epsilon_0$ for the coarse mesh and $0.1123 \times 10^8 \epsilon_0$ for

the fine mesh, indicating convergence. Figures 9 and 10 show the computed stress distribution along the ply interface at $y = h$. Figure 9 indicates ever-decreasing (negative) σ_{yy} near the free edge, indicating singular stress. However, σ_{yy} approaches zero as \bar{x} increases. In addition, shear stress σ_{yz} shows an ever-increasing trend toward the free edge. Other stress components, σ_{xx} , σ_{xy} , σ_{xz} are, of course, zero at the free edge. Shear stress σ_{xz} is almost constant away from the free edge, in accordance with the classical lamination theory. It attains maximum near the free edge before it drops to zero. The normal stress σ_{xx} also reaches maximum near the free edge and then quickly reduces to zero at the free edge itself. The result for shear stress σ_{xy} is not presented here because its magnitude is very small compared with other components.

Figure 11 shows σ_{yy} along the free edge. Here we observe a sharp change in magnitude near the ply interface. This behavior is consistent with the existence of stress singularity. The results presented here agree with those in reference 13. However, in reference 13, an extremely fine mesh had to be used, and the exact nature of stress singularity could not be determined within reasonable accuracy.

4. CONCLUSION

Numerical results indicate that the hybrid finite element formulation involving a special element with embedded stress singularity is a very efficient means for accurate determination of interlaminar stress distribution. For both cross ply and angle ply symmetric laminates considered here, the present method provides converged stress values near the junction of the stress-free edge and the ply interface. These stress values are much more accurate than those obtained by others using conventional finite element models that do not include proper singularity. With the present formulation, it is possible to use a much more coarse finite element mesh, resulting in a substantial improvement in computing effort.

REFERENCES

1. Pipes, R.B., Kaminski, B.E. and Pagano, N.J., "Influence of the Free Edge Upon the Strength of Angle Ply Laminates," ASTM 521, 1973, pp. 218.
2. Whitney, J.M. and Browning, C.E., "Free Edge Delamination of Tensile Coupons," J. Comp. Materials, Vol. 6, April 1972, pp. 300-303.
3. Pagano, N.J. and Pipes, R.B., "Some Observations on the Interlaminar Strength of Composite Laminates," Int. J. Mech. Sci., Vol. 15, 1973, pp. 679.
4. Harris, O. and Orringer, O., "Investigation of Angle Ply Delamination Specimen for Interlaminar Strength Test," J. Comp. Materials, Vol. 12, 1978, pp. 285-299.
5. Pipes, R.B. and Pagano, N.J., "Interlaminar Stresses in Composite Laminates Under Uniform Axial Extension," J. Comp. Materials, Vol. 4, 1970, pp. 538-548.
6. Tang, S., "A Boundary Layer Theory - Part I: Laminated Composites in Plane Stress," J. Comp. Materials, Vol. 9, 1975, pp. 33-41.
7. Hsu, P.W. and Herakovich, C.T., "A Perturbation Solution for Interlaminar Stresses in Bi-directional Laminates," ASTM STP 617, 1977.
8. Wang, J.T.S and Dickson, J.N., "Interlaminar Stresses in Symmetric Composite Laminates," J. Comp. Materials, Vol. 12, 1978, pp. 390-402.
9. Wang, A.S.D. and Crossman, F.W., "Some New Results on Edge Effect in Symmetric Composite Laminates," J. Comp. Materials, Vol. 11, 1977, pp. 92-106.
10. Wang, A.S.D. and Crossman, F.W., "Stress Field Induced by Transient Moisture Sorption in Finite-Width Composite Laminates," J. Comp. Materials, Vol. 12, 1978, pp. 2-18.

11. Rybicki, E.F. and Schmuser, D.W., "Effect of Stacking Sequence and Layup Angle on Free Edge Stresses Around a Hole in a Laminated Plate Under Tension," J. Comp. Materials, Vol. 12, 1978, pp. 300-313.
12. Spilker, R.L. and Chou, S.C., "Edge Effect in Symmetric Composite Laminates: Importance of Satisfying the Traction-Free-Edge Condition," J. Comp. Materials, Vol. 14, 1980, pp. 2-20.
13. Raju, I.S. and Crews, J.H., "Interlaminar Stress Singularities at a Straight Free Edge in Composite Laminates," Computers and Structures, Vol. 14, No. 1-2, 1981, pp. 21-28.
14. Mikhailov, S.E., "Stress Singularity in the Neighborhood of Edge in a Composite Inhomogeneous Anisotropic Body and Some Applications to Composites," Mekhanika Tverdogo Tela, Vol. 14, No. 5, 1979, pp. 103-110.
15. Mikhailov, S.E., "A Two-Dimensional Problem for Two Joined Anisotropic Wedges," Mekhanika Tverdogo Tela, Vol. 13, No. 4, 1978, pp. 155-159.
16. Ting, T.C.T. and Chou, S.C., "Edge Singularities in Anisotropic Composites," Int. J. Solids and Structures, Vol. 17, 1981, pp. 1057-1068.
17. Wang, S.S. and Choi, I., "Boundary Layer Effects in Composites: Part I and II," J. Appl. Mech., Vol. 49, 1982, pp. 541-560.
18. Pian, T.H.H., Tong, P. and Luk, C.H., "Elastic Crack Analysis by a Finite Element Hybrid Method," 3rd Air Force Conf. Matrix. Meth. Struct. Mech., Dayton, Ohio, 1971.
19. Tong, P., Pian, T.H.H. and S. Lasry, "Hybrid Element Approach to Crack Problems in Plane Elasticity," Int. J. Num. Meth. Engng., Vol. 7, 1973, pp. 297-308.
20. Pian, T.H.H., "Crack Elements," Proc. World Congress on Finite Element Methods in Structural Mechanics, Dorset, England, Oct. 1975.

21. Atluri, S.N., Kobayashi, A.S. and Nakagaki, M., "Fracture Mechanics Application of an Assumed Displacement Hybrid Finite Element Procedure," AIAA J., Vol. 13, No. 6, 1975, pp. 734-739.
22. Lin, K.Y. and Mar, J.W., "Finite Element Analysis of Stress Intensity Factors for Cracks at a Bi-Material Interface," Int. J. Fract., Vol. 12, No. 4, 1976, pp. 521-531.
23. Lekhnitskii, S.G., Theory of Elasticity of an Anisotropic Elastic Body, Holden Day, San Francisco, 1965.
24. Pian, T.H.H., "Derivation of Element Stiffness Matrices by Assumed Stress Distribution," AIAA J., Vol. 2, 1964, pp. 1333-1336.
25. Pian, T.H.H. and Tong, P., "Finite Element Methods in Continuum Mechanics," Advances in Applied Mechanics, Vol. 12, 1972, Academic Press, N.Y., pp. 1-58.
26. Tong, P. and Pian, T.H.H., "On the Convergence of the Finite Element Method for Problems with Singularity," Int. J. Solids and Structures, Vol. 9, 1973, pp. 313-321.

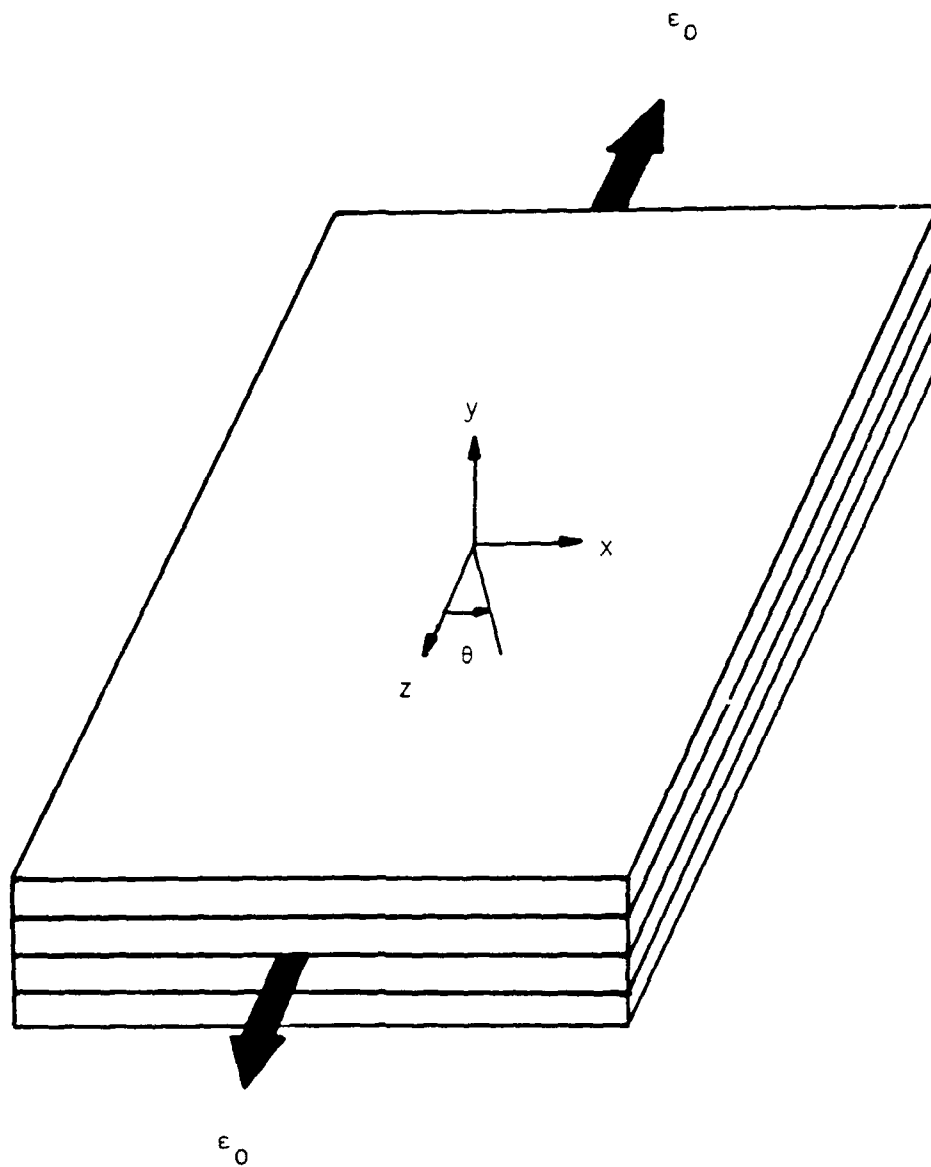


Fig. 1. A symmetric composite laminate under uniform uniaxial strain.

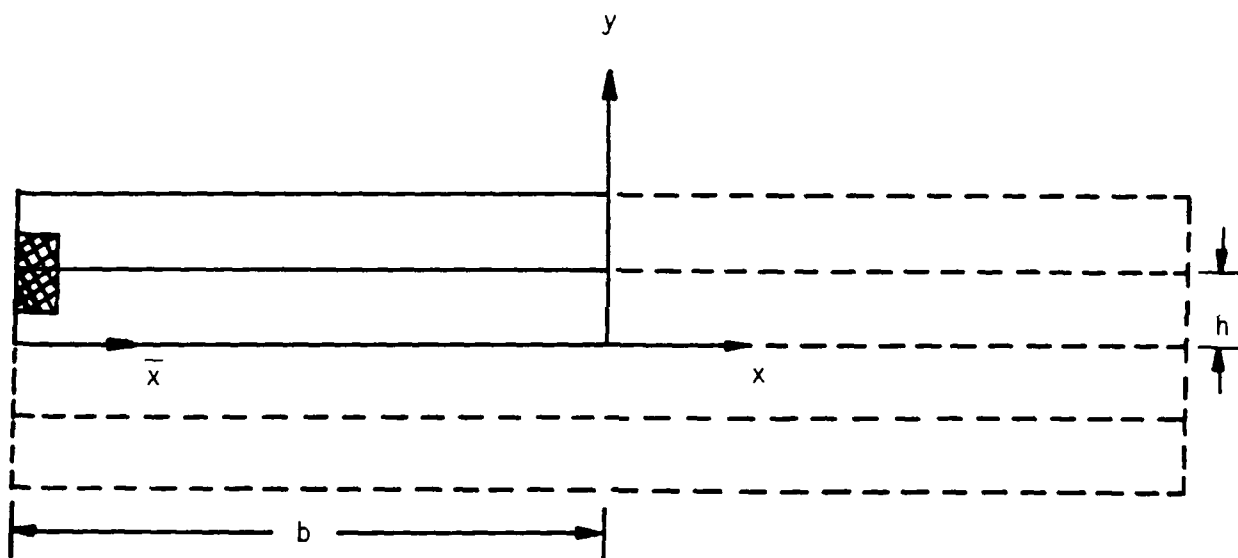


Fig. 2. A quarter of the section modeled.

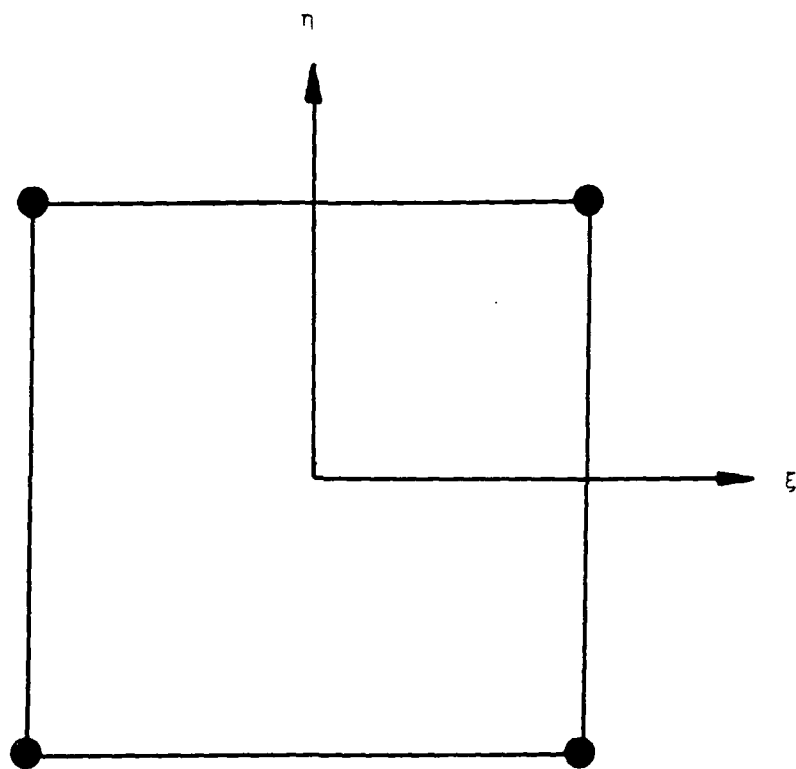


Fig. 3. Four-node regular hybrid element.

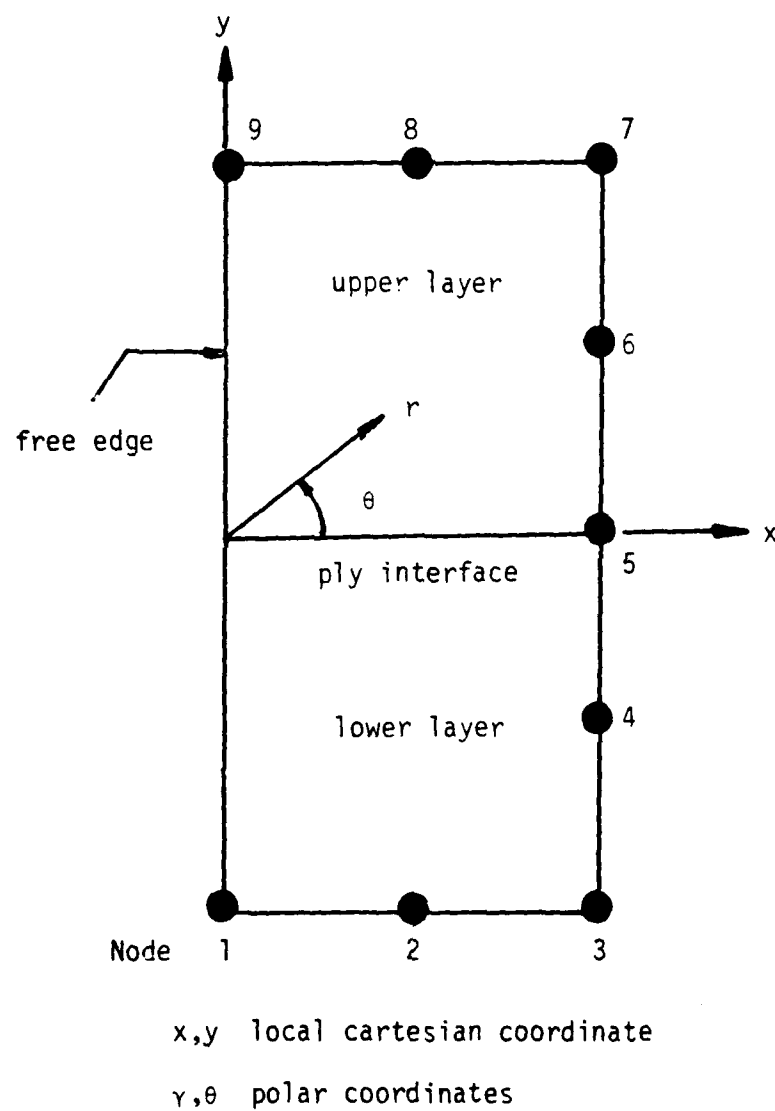


Fig. 4 Nine-node special singular hybrid element.

45°
-45°
-45°
45°

0°
90°
90°
0°

90°
0°
0°
90°

Fig. 5 Cross ply and angle ply laminates

— coarse mesh

— } coarse and fine mesh
- - -

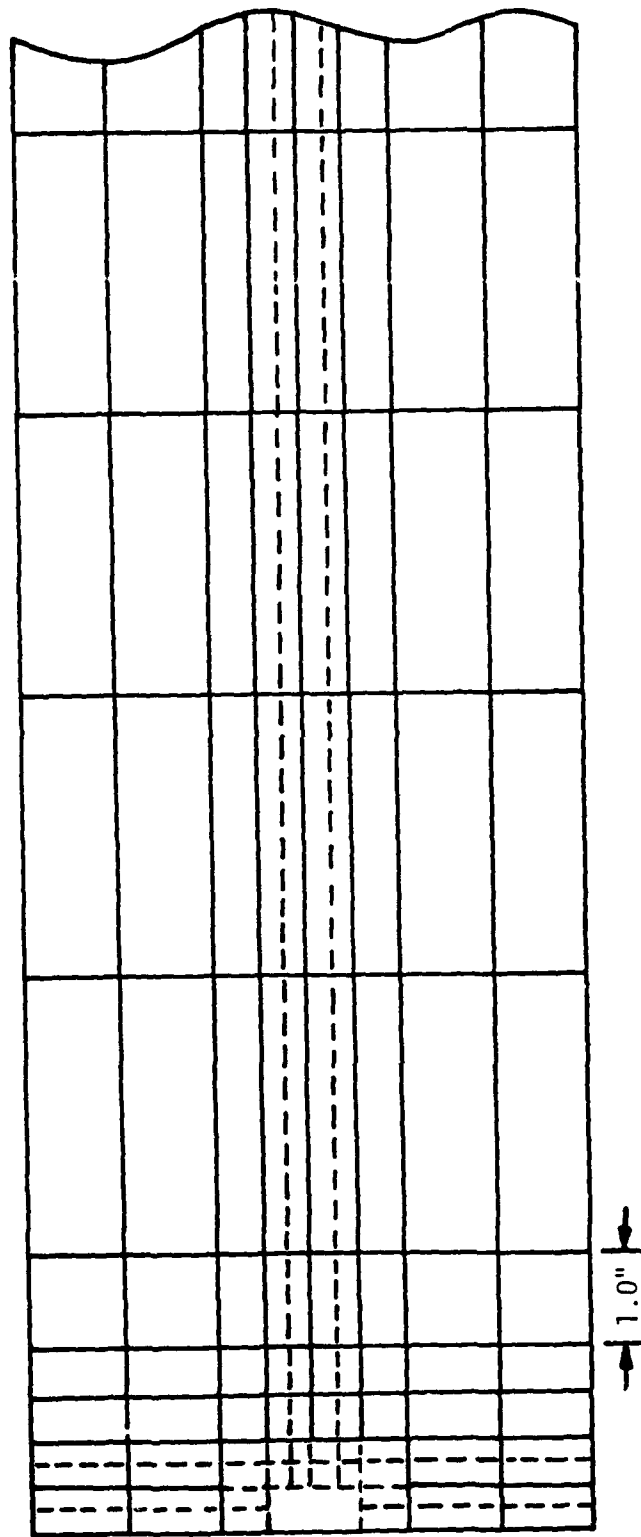


Fig. 6 Finite element model - coarse and fine

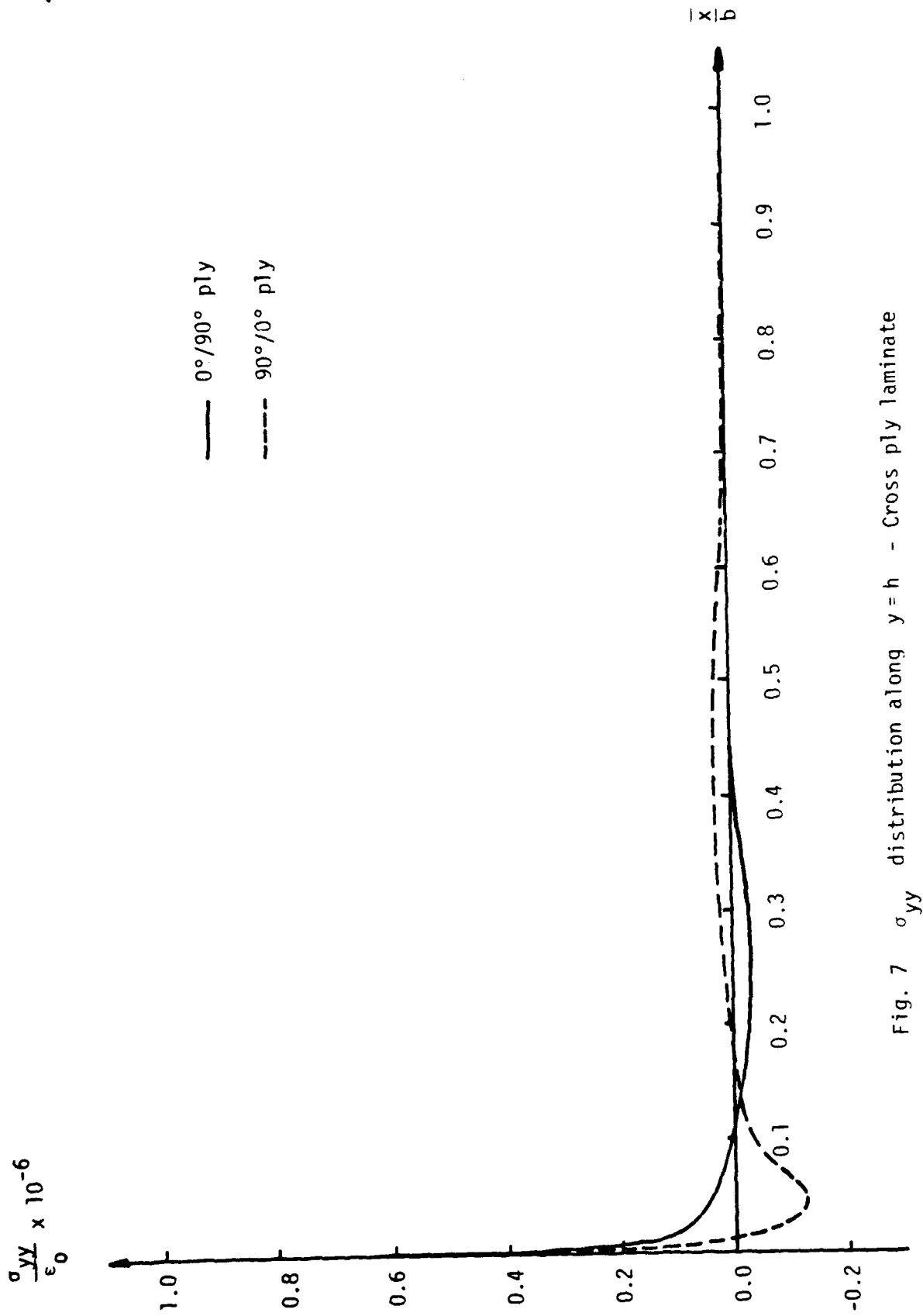


Fig. 7 σ_{yy} distribution along $y=h$ - Cross ply laminate

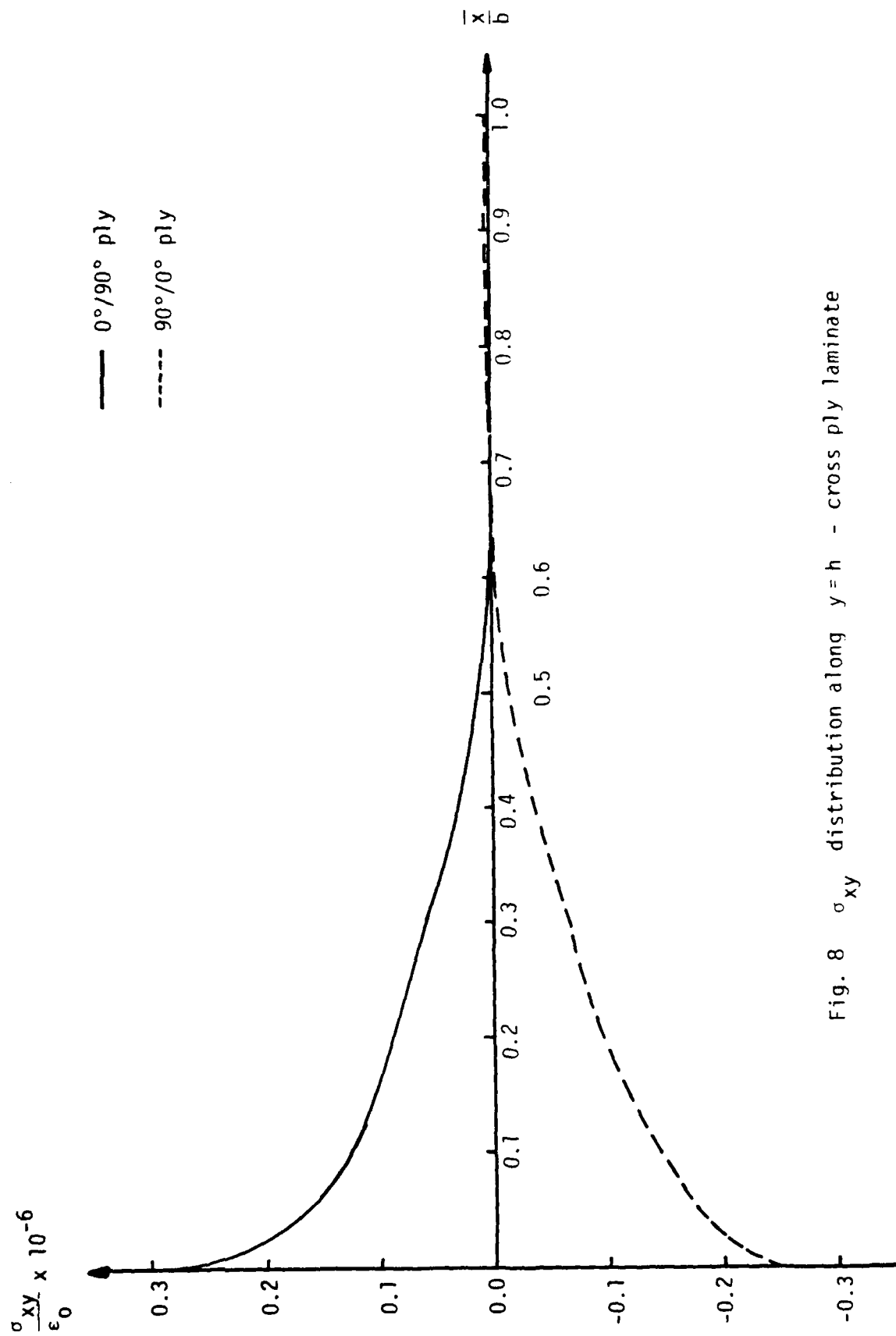


Fig. 8 σ_{xy} distribution along $y=h$ - cross ply laminate

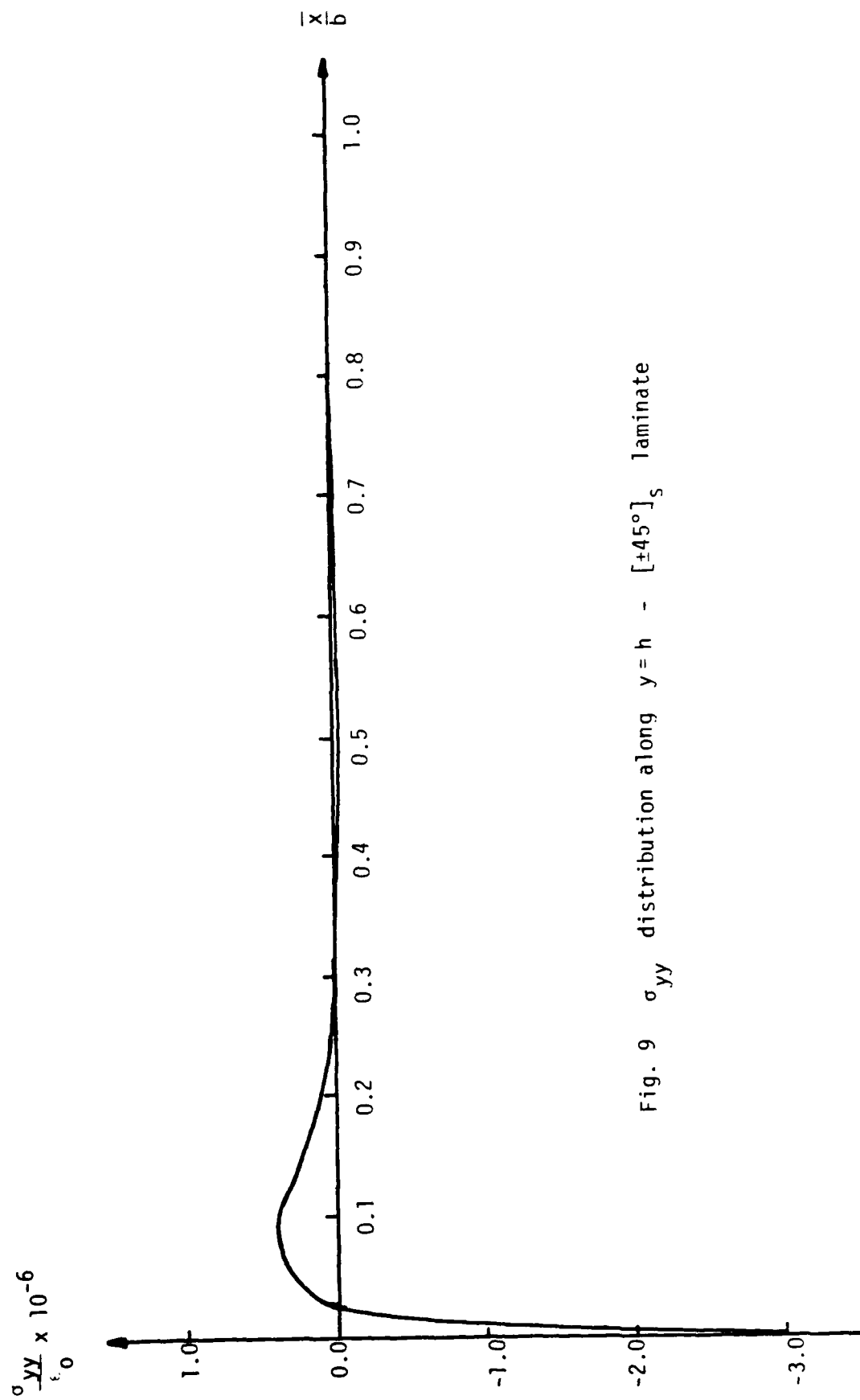


Fig. 9 σ_{yy} distribution along $y = h - [\pm 45^\circ]_s$ laminate

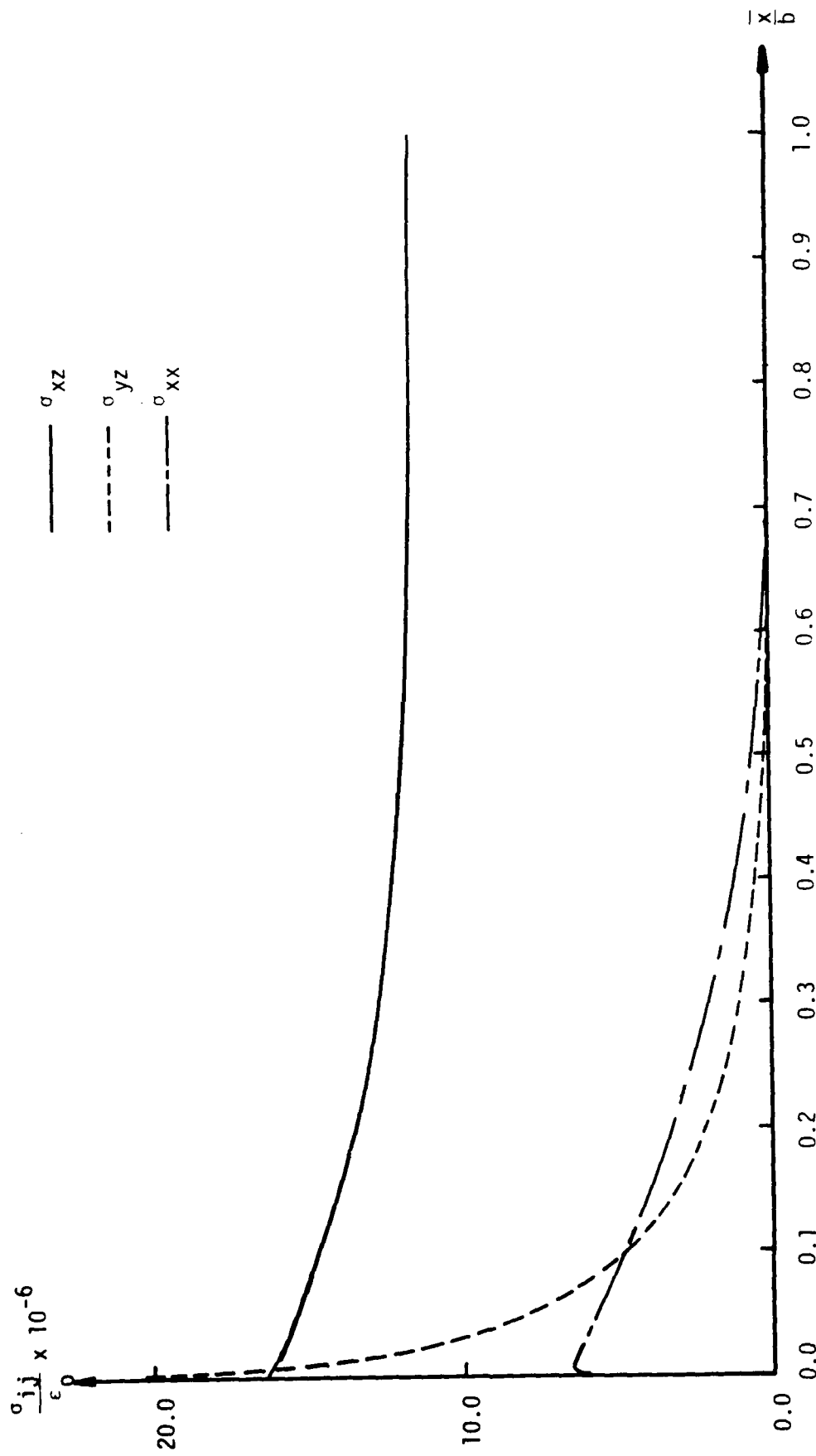


Fig. 10 σ_{xx} , σ_{xz} and σ_{yz} along $y=h$ - $[\pm 45^\circ]_s$ laminate

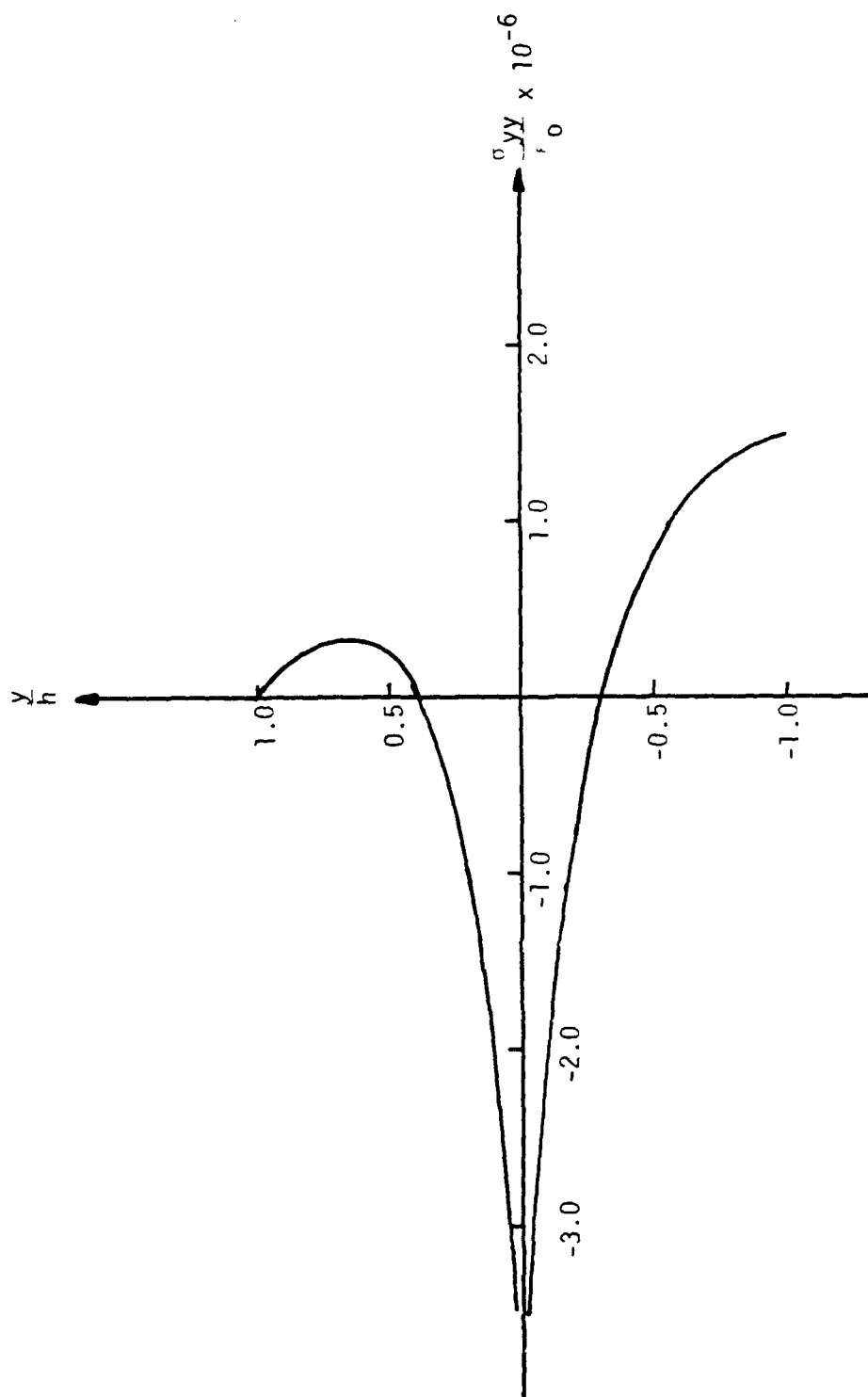


Fig. 11 σ_{yy} along the free edge - $[\pm 45^\circ]_s$ laminate

APPENDIX

A.1 ANISOTROPIC ELASTICITY WITH PRESCRIBED UNIFORM UNIAXIAL STRAIN

For three-dimensional solids, the three equations of equilibrium are expressed in terms of stress components $\sigma_{xx}, \sigma_{yy}, \dots, \sigma_{xy}$;

$$\frac{\partial \sigma_{xx}}{\partial x} + \frac{\partial \sigma_{xy}}{\partial y} + \frac{\partial \sigma_{xz}}{\partial z} = 0$$

$$\frac{\partial \sigma_{xy}}{\partial x} + \frac{\partial \sigma_{yy}}{\partial y} + \frac{\partial \sigma_{yz}}{\partial z} = 0$$

(A.1.1)

$$\frac{\partial \sigma_{xz}}{\partial x} + \frac{\partial \sigma_{yz}}{\partial y} + \frac{\partial \sigma_{zz}}{\partial z} = 0$$

The six strain components $\epsilon_{xx}, \epsilon_{yy}, \dots, \epsilon_{xy}$ are related to the six stress components as follows:

$$\epsilon_{xx} = S_{11} \sigma_{xx} + S_{12} \sigma_{yy} + S_{13} \sigma_{zz} + S_{14} \sigma_{yz} + S_{15} \sigma_{zx} + S_{16} \sigma_{xy}$$

$$\epsilon_{yy} = S_{21} \sigma_{xx} + S_{22} \sigma_{yy} + S_{23} \sigma_{zz} + S_{24} \sigma_{yz} + S_{25} \sigma_{zx} + S_{26} \sigma_{xy}$$

$$\epsilon_{zz} = S_{31} \sigma_{xx} + S_{32} \sigma_{yy} + S_{33} \sigma_{zz} + S_{34} \sigma_{yz} + S_{35} \sigma_{zx} + S_{36} \sigma_{xy}$$

$$\epsilon_{yz} = S_{41} \sigma_{xx} + S_{42} \sigma_{yy} + S_{43} \sigma_{zz} + S_{44} \sigma_{yz} + S_{45} \sigma_{zx} + S_{46} \sigma_{xy}$$

$$\epsilon_{zx} = S_{51} \sigma_{xx} + S_{52} \sigma_{yy} + S_{53} \sigma_{zz} + S_{54} \sigma_{yz} + S_{55} \sigma_{zx} + S_{56} \sigma_{xy}$$

$$\epsilon_{xy} = S_{61} \sigma_{xx} + S_{62} \sigma_{yy} + S_{63} \sigma_{zz} + S_{64} \sigma_{yz} + S_{65} \sigma_{zx} + S_{66} \sigma_{xy}$$

(A.1.2)

where S_{11} , S_{12} etc. are compliance coefficients. The strain-displacement relation is expressed as

$$\begin{aligned}
 \epsilon_{xx} &= \frac{\partial u}{\partial x} \\
 \epsilon_{yy} &= \frac{\partial v}{\partial y} \\
 \epsilon_{zz} &= \frac{\partial w}{\partial z} \\
 \epsilon_{yz} &= \frac{\partial v}{\partial z} + \frac{\partial w}{\partial y} \\
 \epsilon_{zx} &= \frac{\partial w}{\partial x} + \frac{\partial u}{\partial z} \\
 \epsilon_{xy} &= \frac{\partial u}{\partial y} + \frac{\partial v}{\partial x}
 \end{aligned} \tag{A.1.3}$$

where u , v and w are displacement components in x , y and z directions respectively.

If the body is subjected to uniform uniaxial strain $\epsilon_{zz} = \epsilon_0$, stress components do not vary along the z direction [23]. Then the equilibrium equation reduces to

$$\begin{aligned}
 \frac{\partial \sigma_{xx}}{\partial x} + \frac{\partial \sigma_{xy}}{\partial y} &= 0 \\
 \frac{\partial \sigma_{xy}}{\partial x} + \frac{\partial \sigma_{yy}}{\partial y} &= 0 \\
 \frac{\partial \sigma_{xz}}{\partial x} + \frac{\partial \sigma_{yz}}{\partial y} &= 0
 \end{aligned} \tag{A.1.4}$$

Now from the third equation of (A.1.2)

$$\sigma_{zz} = \frac{1}{S_{33}} (\epsilon_0 - S_{31} \sigma_{xx} - S_{32} \sigma_{yy} - S_{34} \sigma_{yz} - S_{35} \sigma_{zx} - S_{36} \sigma_{xy}) \tag{A.1.5}$$

Substituting (A.1.5) into the remaining five equations in eq. (A.1.2), we obtain

$$\begin{aligned}
 \epsilon_{xx} &= B_{11}\sigma_{xx} + B_{12}\sigma_{yy} + B_{14}\sigma_{yz} + B_{15}\sigma_{zx} + B_{16}\sigma_{xy} + \frac{S_{13}}{S_{33}} \epsilon_0 \\
 \epsilon_{yy} &= B_{21}\sigma_{xx} + B_{22}\sigma_{yy} + B_{24}\sigma_{yz} + B_{25}\sigma_{zx} + B_{26}\sigma_{xy} + \frac{S_{23}}{S_{33}} \epsilon_0 \\
 \epsilon_{yz} &= B_{41}\sigma_{xx} + B_{42}\sigma_{yy} + B_{44}\sigma_{yz} + B_{45}\sigma_{zx} + B_{46}\sigma_{xy} + \frac{S_{43}}{S_{33}} \epsilon_0 \quad (A.1.6) \\
 \epsilon_{zx} &= B_{51}\sigma_{xx} + B_{52}\sigma_{yy} + B_{54}\sigma_{yz} + B_{55}\sigma_{zx} + B_{56}\sigma_{xy} + \frac{S_{53}}{S_{33}} \epsilon_0 \\
 \epsilon_{xy} &= B_{61}\sigma_{xx} + B_{62}\sigma_{yy} + B_{64}\sigma_{yz} + B_{65}\sigma_{zx} + B_{66}\sigma_{xy} + \frac{S_{63}}{S_{33}} \epsilon_0
 \end{aligned}$$

where

$$B_{ij} = S_{ij} - \frac{S_{i3} S_{j3}}{S_{33}} \quad (i, j = 1, 2, 4, 5, 6) \quad (A.1.7)$$

For symmetric angle ply case

$$\begin{aligned}
 B_{14} &= B_{24} = B_{34} = B_{54} = 0 \\
 B_{16} &= B_{26} = B_{36} = B_{56} = 0
 \end{aligned} \quad (A.1.8)$$

In matrix form, eq. (A.1.6) can be written as

$$\epsilon = B \sigma + \epsilon_0 \quad (A.1.9)$$

with

$$\underline{\epsilon} = \begin{Bmatrix} \epsilon_{xx} \\ \epsilon_{yy} \\ \epsilon_{yz} \\ \epsilon_{zx} \\ \epsilon_{xy} \end{Bmatrix} \quad (\text{A.1.10})$$

$$\underline{B} = \begin{bmatrix} B_{11} & \cdot & \cdot & \cdot & B_{16} \\ & & & & \\ & & & & \\ & & & & \\ B_{61} & \cdot & \cdot & \cdot & B_{66} \end{bmatrix} = 5 \times 5 \text{ matrix} \quad (\text{A.1.11})$$

$$\underline{\sigma} = \begin{Bmatrix} \sigma_{xx} \\ \sigma_{yy} \\ \sigma_{yz} \\ \sigma_{zx} \\ \sigma_{xy} \end{Bmatrix} \quad (\text{A.1.12})$$

$$\underline{\epsilon}_0 = \begin{Bmatrix} s_{13} \\ s_{23} \\ s_{43} \\ s_{53} \\ s_{63} \end{Bmatrix} \frac{\epsilon_0}{s_{33}} \quad (\text{A.1.13})$$

For the present problem, the displacement components u, v, w can be expressed as

$$\begin{aligned} u &= U(x,y) \\ v &= V(x,y) \\ w &= \epsilon_0 z + W(x,y) \end{aligned} \tag{A.1.14}$$

Then the strain-displacement relation is written as

$$\begin{aligned} \epsilon_{xx} &= \frac{\partial U}{\partial x} \\ \epsilon_{yy} &= \frac{\partial V}{\partial y} \\ \epsilon_{yz} &= \frac{\partial W}{\partial y} \\ \epsilon_{zx} &= \frac{\partial W}{\partial x} \\ \epsilon_{xy} &= \frac{\partial U}{\partial y} + \frac{\partial V}{\partial x} \end{aligned} \tag{A.1.15}$$

For cross ply laminate, further simplification is possible since

$$\begin{aligned} \sigma_{yz} &= \sigma_{zx} = 0 \\ \epsilon_{yz} &= \epsilon_{zx} = 0 \end{aligned} \tag{A.1.16}$$

The equilibrium equation now reduces to

$$\frac{\partial \sigma_{xx}}{\partial x} + \frac{\partial \sigma_{xy}}{\partial y} = 0$$

(A.1.17)

$$\frac{\partial \sigma_{xy}}{\partial x} + \frac{\partial \sigma_{yy}}{\partial y} = 0$$

Also

$$\epsilon_{xx} = B_{11} \sigma_{xx} + B_{12} \sigma_{yy} + \frac{S_{13}}{S_{33}} \epsilon_0$$

$$\epsilon_{yy} = B_{21} \sigma_{xx} + B_{22} \sigma_{yy} + \frac{S_{23}}{S_{33}} \epsilon_0 \quad (\text{A.1.18})$$

$$\epsilon_{xy} = B_{66} \sigma_{xy}$$

and

$$\epsilon_{xx} = \frac{\partial U}{\partial x}$$

$$\epsilon_{yy} = \frac{\partial V}{\partial y}$$

(A.1.19)

$$\epsilon_{xy} = \frac{\partial U}{\partial y} + \frac{\partial V}{\partial x}$$

A.2 CONSTANT STRESS FIELD**

The role of predetermined constant stress field is to separate terms involving prescribed strain ϵ_0 from the assumed stress field and the corresponding assumed displacement field. For the present special element, the constant stress term satisfies the stress-free condition along the free edge. In addition, the constant stress field and the displacement field integrated from the constant stress field satisfy the bonding condition along the ply interface.

A.2.1 Cross-Ply Case

For the coordinate system shown in figure 4, the stress-free conditions are:

$$\sigma_{xx}^u = \sigma_{xy}^u = 0 \quad (A.2.1)$$

at $\theta = \frac{\pi}{2}$

and

$$\sigma_{xx}^l = \sigma_{xy}^l = 0 \quad (A.2.2)$$

at $\theta = -\frac{\pi}{2}$

The bonding condition along $\theta = 0^\circ$ are

$$\begin{aligned} \sigma_{xy}^u &= \sigma_{xy}^l \\ \sigma_{yy}^u &= \sigma_{yy}^l \\ U^u &= U^l \\ V^u &= V^l \end{aligned} \quad (A.2.3)$$

** The senior author has recently noticed a similar development in ref. 17.

The superscripts u and l stand for the upper layer and the lower layer respectively. The constant stress components ${}^0\sigma_{xx}$, ${}^0\sigma_{yy}$, ${}^0\sigma_{xy}$ that satisfy the above stress-free and the bonding conditions are

$$\begin{aligned} {}^0\sigma_{xx}^u &= {}^0\sigma_{yy}^l = 0 \\ {}^0\sigma_{xy}^u &= {}^0\sigma_{xy}^l = 0 \\ {}^0\sigma_{yy}^u &= {}^0\sigma_{yy}^l = c \end{aligned} \tag{A.2.4}$$

where c is a constant to be determined as follows. Substituting the constant stress terms in eq. (A.2.4) into eq. (A.1.18) and integrating, we obtain the corresponding displacement components ${}^0U^u$ and ${}^0V^u$ for the upper layer as follows

$$\begin{aligned} {}^0U^u &= (B_{12}^u c + \frac{S_{13}^u}{S_{33}^u} \epsilon_0) x \\ {}^0V^u &= (B_{22}^u c + \frac{S_{23}^u}{S_{33}^u} \epsilon_0) y \end{aligned} \tag{A.2.5}$$

excluding the rigid body modes. Similar expression holds for displacement components ${}^0U^l$ and ${}^0V^l$. Then from the displacement continuity at the $90^\circ - 0^\circ$ ply interface.

$$(B_{12}^u c + \frac{S_{13}^u}{S_{33}^u} \epsilon_0) x = (B_{12}^l c + \frac{S_{13}^l}{S_{33}^l} \epsilon_0) x \tag{A.2.6}$$

Solving for c , we obtain

$$c = \frac{\epsilon_0}{B_{12}^u - B_{12}^l} \left(\frac{S_{13}^l}{S_{33}^l} - \frac{S_{13}^u}{S_{33}^u} \right) \quad (\text{A.2.7})$$

A.2.2 Angle-Ply Case

Now stress-free conditions are:

$$\sigma_{xx}^u = \sigma_{xy}^u = \sigma_{xz}^u = 0 \quad (\text{A.2.8})$$

at $\theta = \frac{\pi}{2}$

and

$$\sigma_{xx}^l = \sigma_{xy}^l = \sigma_{xz}^l = 0 \quad (\text{A.2.9})$$

at $\theta = -\frac{\pi}{2}$

The bonding conditions along the ply interface ($\theta = 0^\circ$) are;

$$\begin{aligned} \sigma_{xy}^u &= \sigma_{xy}^l \\ \sigma_{yy}^u &= \sigma_{yy}^l \\ \sigma_{yz}^u &= \sigma_{yz}^l \end{aligned} \quad (\text{A.2.10})$$

and

$$\begin{aligned} U^u &= U^l \\ V^u &= V^l \\ W^u &= W^l \end{aligned} \quad (\text{A.2.11})$$

The constant stress components that satisfy the above stress-free and the bonding conditions are

$$\begin{aligned}
 \sigma_{yy}^u &= \sigma_{yy}^l = c_1 \\
 \sigma_{yz}^u &= \sigma_{yz}^l = c_2 \\
 \sigma_{xy}^u &= \sigma_{xy}^l = 0 \\
 \sigma_{xz}^u &= \sigma_{xz}^l = 0 \\
 \sigma_{xx}^u &= \sigma_{xx}^l = 0
 \end{aligned} \tag{A.2.12}$$

Substituting this stress state into eq. (A.1.15) and integrating, we obtain the corresponding displacement fields. Then from the matching condition eq. (A.2.11) of displacements along the ply interface

$$c_2 = 0 \tag{A.2.13}$$

and

$$c_1 = \sigma_{yy}^u = \sigma_{yy}^l = - \frac{\epsilon_0}{(B_{52}^u - B_{52}^l)} \left(\frac{S_{53}^u}{S_{33}^u} - \frac{S_{53}^l}{S_{53}^l} \right) \tag{A.2.14}$$

or since

$$\begin{aligned}
 B_{52}^u &= - B_{52}^l \\
 S_{53}^u &= - S_{53}^l \\
 S_{33}^u &= S_{33}^l
 \end{aligned} \tag{A.2.15}$$

for symmetric angle ply,

$$\sigma_{yy}^u = \sigma_{yy}^l = - \frac{\epsilon_0 S_{53}^u}{B_{52}^u S_{33}^u} \quad (A.2.16)$$

In addition,

$$\begin{aligned} u^u &= (B_{12}^u \sigma_{yy}^u + \frac{S_{13}^u}{S_{33}^u} \epsilon_0) x \\ v^u &= (B_{22}^u \sigma_{yy}^u + \frac{S_{23}^u}{S_{33}^u} \epsilon_0) y \end{aligned} \quad (A.2.17)$$

$$w^u = 0$$

Similar expressions hold for stress $\sigma_{xx}^l \dots \sigma_{xy}^l$ and displacement u^l , v^l and w^l for the lower layer.

A.3 ASSUMED STRESS FIELD (SINGULAR AND NONSINGULAR)

The assumed stress and the corresponding displacement fields satisfy all governing equations of elasticity, the stress-free condition over the free edge and the bonding condition along the ply interface. In order to ensure convergence, the assumed stress must include singular terms [26]. The determination of singular stress fields proceeds as follows.

A.3.1 Cross-Ply Case

By introducing a stress function $F(x,y)$ such that

$$\begin{aligned}\sigma_{xx} &= \frac{\partial^2 F}{\partial y^2} \\ \sigma_{yy} &= \frac{\partial^2 F}{\partial x^2} \\ \sigma_{xy} &= - \frac{\partial^2 F}{\partial x \partial y}\end{aligned}\tag{A.3.1}$$

the equilibrium equation (A.1.17) is always satisfied, and the compatibility among strain components in eq. (A.1.18) leads to the following fourth-order equation for F .

$$B_{22} \frac{\partial^4 F}{\partial x^4} + (2 B_{12} + B_{66}) \frac{\partial^4 F}{\partial x^2 \partial y^2} + B_{11} \frac{\partial^4 F}{\partial y^4} = 0\tag{A.3.2}$$

The above equation has the general solution of the following form:

$$F(x,y) = F_k (x + \mu_k y) \quad (k = 1,2,3,4) \tag{A.3.3}$$

where μ_k is a root of the following fourth order algebraic equation.

$$B_{11} \mu^4 + (2 B_{12} + B_{66}) \mu^2 + B_{22} = 0 \quad (A.3.4)$$

The solutions to the above equations constitute two conjugate pairs. Thus if μ_1 and μ_2 are two distinct roots, then

$$\begin{aligned} \mu_3 &= \overline{\mu_1} \\ \mu_4 &= \overline{\mu_2} \end{aligned} \quad (A.3.5)$$

where $\overline{\mu_1}$ is the conjugate of μ_1 etc. In order to determine the singular stress field and also the non-singular stress fields, we express F_k as

$$F_k(x + \mu_k y) = A_k \frac{(x + \mu_k y)^{\alpha+2}}{(\alpha+2)(\alpha+1)} \quad (A.3.6)$$

where A_k is a coefficient and α is a quantity to be determined by an eigenvalue analysis. The local coordinates x and y are related to the polar coordinates r and θ as follows (fig. 4).

$$\begin{aligned} x &= r \cos \theta \\ y &= r \sin \theta \end{aligned} \quad (A.3.7)$$

Then

$$x + \mu_k y = r C_k \quad (A.3.8)$$

where

$$C_k = \cos \theta + \mu_k \sin \theta \quad (A.3.9)$$

From eq. (A.3.1), the non-constant stress components are expressed as

$$\begin{aligned}
 *_{\sigma_{xx}}^u &= r^\alpha \sum_{k=1}^4 A_k^u (\mu_k^u)^2 (C_k^u)^\alpha \\
 *_{\sigma_{yy}}^u &= r^\alpha \sum_{k=1}^4 A_k^u (C_k^u)^\alpha \\
 *_{\sigma_{xy}}^u &= - r^\alpha \sum_{k=1}^4 A_k^u \mu_k^u (C_k^u)^\alpha
 \end{aligned} \tag{A.3.10}$$

for the upper layer. The corresponding displacement components are determined by integrating eq. (A.1.18)

$$\begin{aligned}
 *U^u &= \frac{r^{\alpha+1}}{\alpha+1} \sum_{k=1}^4 A_k^u p_k^u (C_k^u)^{\alpha+1} \\
 *V^u &= \frac{r^{\alpha+1}}{\alpha+1} \sum_{k=1}^4 A_k^u q_k^u (C_k^u)^{\alpha+1}
 \end{aligned} \tag{A.3.11}$$

where

$$\begin{aligned}
 p_k &= B_{11} \mu_k^2 + B_{12} \\
 q_k &= B_{12} \mu_k + B_{22}/\mu_k
 \end{aligned} \tag{A.3.12}$$

Similar expression holds for the lower layer. Note that ϵ_0 term does not appear in the above equation since it was taken into account by the constant stress field and the corresponding displacement in the previous section.

Applying the bonding condition along $\theta = 0$,

$$\sum_{k=1}^4 A_k^u (C_k^u)^\alpha = \sum_{k=1}^4 A_k^l (C_k^l)^\alpha$$

$$\sum_{k=1}^4 A_k^u \mu_k^u (C_k^u)^\alpha = \sum_{k=1}^4 A_k^l \mu_k^l (C_k^l)^\alpha$$

(A.3.13)

$$\sum_{k=1}^4 A_k^u p_k^u (C_k^u)^{\alpha+1} = \sum_{k=1}^4 A_k^l p_k^l (C_k^l)^{\alpha+1}$$

$$\sum_{k=1}^4 A_k^u q_k^u (C_k^u)^{\alpha+1} = \sum_{k=1}^4 A_k^l q_k^l (C_k^l)^{\alpha+1}$$

The above equation can be rewritten in matrix form as

$$\underline{A}^u = \underline{I} \underline{A}^l \quad (A.3.14)$$

where

$$\underline{A}^u = \begin{Bmatrix} A_1^u \\ A_2^u \\ A_3^u \\ A_4^u \end{Bmatrix} \quad (A.3.15)$$

$$\underline{A}^{\ell} = \begin{Bmatrix} A_1^{\ell} \\ A_2^{\ell} \\ A_3^{\ell} \\ A_4^{\ell} \end{Bmatrix} \quad (\text{A.3.16})$$

and \underline{I} is a 4×4 matrix. Since $\star_{\sigma_{xx}}^u = \star_{\sigma_{xy}}^u = 0$ at $\theta = \frac{\pi}{2}$ ($\cos\theta = 0$, $\sin\theta = 1$),

$$\sum_{k=1}^4 A_k^u (\mu_k^u)^{2+\alpha} = 0 \quad (\text{A.3.17})$$

$$\sum_{k=1}^4 A_k^u (\mu_k^u)^{1+\alpha} = 0$$

And also $\star_{\sigma_{xx}}^{\ell} = \star_{\sigma_{xy}}^{\ell} = 0$ at $\theta = -\frac{\pi}{2}$ ($\cos\theta = 0$, $\sin\theta = -1$)

$$\sum_{k=1}^4 A_k^{\ell} (-\mu_k^{\ell})^{2+\alpha} = 0 \quad (\text{A.3.18})$$

$$\sum_{k=1}^4 A_k^{\ell} (-\mu_k^{\ell})^{1+\alpha} = 0$$

Equations (A.3.17) and (A.3.18), in conjunction with eq. (A.3.14), leads to a system of homogeneous equations for \underline{A}^u as:

$$\zeta(\alpha) \underline{A}^u = 0 \quad (\text{A.3.19})$$

where $\zeta(\alpha)$ is 4×4 matrix with the unknown α . For nontrivial \underline{A}^u , the determinant of $\zeta(\alpha)$ must be equal to zero, which leads to an eigenvalue problem. The eigenvalue α can be either real or complex. For singular stress,

$$-1 < \text{Re}(\alpha) < 0 \quad (\text{A.3.20})$$

where $\text{Re}(\alpha)$ is the real part of α . For the material properties used in the present problem, the first eigenvalue corresponding to stress singularity is $\alpha = -0.333888$.

Using eigenvalues and eigenvectors determined from eigenvalue analysis, we may construct the assumed stress and displacement field as follows:

$$\begin{aligned} \sigma_{xx}^u &= \sum_{i=1}^n r^{\alpha_i} \text{Re} \left[\sum_{k=1}^4 (A_k^u)_{\alpha=\alpha_i} (\nu_k^u)^2 (C_k^u)^{\alpha_i} \right] \varepsilon_i \\ \sigma_{yy}^u &= \sum_{i=1}^n r^{\alpha_i} \text{Re} \left[\sum_{k=1}^4 (A_k^u)_{\alpha=\alpha_i} (C_k^u)^{\alpha_i} \right] \varepsilon_i \\ \sigma_{xy}^u &= - \sum_{i=1}^n r^{\alpha_i} \text{Re} \left[\sum_{k=1}^4 (A_k^u)_{\alpha=\alpha_i} \nu_k^u (C_k^u)^{\alpha_i} \right] \varepsilon_i \end{aligned} \quad (\text{A.3.21})$$

and

$$\begin{aligned}
 *U^u &= \sum_{i=1}^n \frac{r^{\alpha_i+1}}{\alpha_i+1} \operatorname{Re} \left[\sum_{k=1}^4 (A_k^u)_{\alpha=\alpha_i} p_k^u (C_k^u)^{\alpha_i+1} \right] \beta_i \\
 *V^u &= \sum_{i=1}^n \frac{r^{\alpha_i+1}}{\alpha_i+1} \operatorname{Re} \left[\sum_{k=1}^4 (A_k^u)_{\alpha=\alpha_i} q_k^u (C_k^u)^{\alpha_i+1} \right] \beta_i
 \end{aligned} \tag{A.3.22}$$

where β_1, \dots, β_n are unknown free parameters. In the above expression, the following relations are utilized.

$$\mu_{k+2} = \overline{\mu_k} \quad (k = 1, 2) \tag{A.3.23}$$

and thus

$$\begin{aligned}
 p_{k+2} &= \overline{p_k} \\
 q_{k+2} &= \overline{q_k} \quad (k = 1, 2) \\
 c_{k+2} &= \overline{c_k}
 \end{aligned} \tag{A.3.24}$$

In the present study, a three term ($n = 3$) approximation was used.

A.3.2 Angle Ply Case

The stress components are now expressed in terms of stress functions $F(x, y)$ and $\psi(x, y)$ such that

$$\sigma_{xx} = \frac{\partial^2 F}{\partial y^2}$$

$$\sigma_{yy} = \frac{\partial^2 F}{\partial x^2}$$

(cont'd)

$$\sigma_{xy} = - \frac{\partial^2 F}{\partial x \partial y}$$

$$\sigma_{xz} = \frac{\partial \psi}{\partial y} \quad (A.3.25)$$

$$\sigma_{yz} = - \frac{\partial \psi}{\partial x}$$

The compatibility among strain components in eq. (A.1.5) leads to the following two homogenous equations for F and ψ :

$$L_4 F + L_3 \psi = 0 \quad (A.3.26a)$$

$$L_3 F + L_2 \psi = 0 \quad (A.3.26b)$$

where the differential operators L_2 , L_3 and L_4 are given as

$$\begin{aligned} L_2 &= B_{44} \frac{\partial^2}{\partial x^2} - 2B_{45} \frac{\partial^2}{\partial x \partial y} + B_{55} \frac{\partial^2}{\partial y^2} \\ L_3 &= -B_{24} \frac{\partial^3}{\partial x^3} + (B_{25} + B_{46}) \frac{\partial^3}{\partial x^2 \partial y} - (B_{14} + B_{56}) \frac{\partial^3}{\partial x \partial y^2} + B_{15} \frac{\partial^3}{\partial y^3} \\ L_4 &= B_{22} \frac{\partial^4}{\partial x^4} - 2B_{26} \frac{\partial^4}{\partial x^3 \partial y} + (2B_{12} + B_{66}) \frac{\partial^4}{\partial x^2 \partial y^2} \\ &\quad - 2B_{16} \frac{\partial^4}{\partial x \partial y^3} + B_{11} \frac{\partial^4}{\partial y^4} \end{aligned} \quad (A.3.27)$$

Combining eqs. (A.3.26a) and (A.3.26b) leads to

$$(L_4 L_2 - L_3^2) F = 0 \quad (\text{A.3.28})$$

The above equation has the general solution of the form

$$F(x,y) = F_k (x + \mu_k y) \quad (k = 1, 2, \dots, 6) \quad (\text{A.3.29})$$

where μ_k is a root of the following sixth order equation;

$$\ell_4(\mu) \ell_2(\mu) - \ell_3^2(\mu) = 0 \quad (\text{A.3.30})$$

with

$$\begin{aligned} \ell_2(\mu) &= B_{55} \mu^2 - 2B_{45} \mu + B_{44} \\ \ell_3(\mu) &= B_{15} \mu^3 - (B_{14} + B_{56}) \mu^2 + (B_{25} + B_{46}) \mu - B_{24} \\ \ell_4(\mu) &= B_{11} \mu^4 - 2B_{16} \mu^3 + (2B_{12} + B_{66}) \mu^2 - 2B_{26} \mu + B_{22} \end{aligned} \quad (\text{A.3.31})$$

The solutions to the eq. (A.3.30) constitute three conjugate pairs. Therefore if μ_1 , μ_2 and μ_3 are three distinct roots, then

$$\mu_{k+3} = \overline{\mu_k} \quad (k = 1, 2, 3) \quad (\text{A.3.32})$$

Also from eq. (A.3.26b) the solution for ψ_k can be expressed as

$$\psi_k(x + \mu_k y) = -\lambda_k \frac{d F_k(x + \mu_k y)}{d(x + \mu_k y)} \quad (\text{A.3.33})$$

where

$$\lambda_k = -\frac{\ell_3(\mu_k)}{\ell_2(\mu_k)} \quad (\text{A.3.34})$$

Again, using polar coordinates r and θ (fig. 4)

$$x + \mu_k y = r (\cos \theta + \mu_k \sin \theta) = r C_k \quad (\text{A.3.35})$$

where

$$C_k = \cos \theta + \mu_k \sin \theta \quad (\text{A.3.36})$$

Introducing F_k and ψ_k into eq. (A.3.25)

$$\begin{aligned} *_{\sigma_{xx}}^u &= r^\alpha \sum_{k=1}^6 A_k^u (\mu_k^u)^2 (C_k^u)^\alpha \\ *_{\sigma_{yy}}^u &= r^\alpha \sum_{k=1}^6 A_k^u (C_k^u)^\alpha \\ *_{\sigma_{xy}}^u &= -r^\alpha \sum_{k=1}^6 A_k^u \mu_k^u (C_k^u)^\alpha \\ *_{\sigma_{xz}}^u &= r^\alpha \sum_{k=1}^6 A_k^u \lambda_k^u \mu_k^u (C_k^u)^\alpha \\ *_{\sigma_{yz}}^u &= -r^\alpha \sum_{k=1}^6 A_k^u \lambda_k^u (C_k^u)^\alpha \end{aligned} \quad (\text{A.3.37})$$

The corresponding displacements are determined by integrating eq. (A.1.6) without ϵ_0 terms. They are written as

$$*U^u = \frac{r^{\alpha+1}}{\alpha+1} \sum_{k=1}^6 A_k^u p_k^u (C_k^u)^{\alpha+1} \quad (\text{cont'd})$$

$$*V^u = \frac{r^{\alpha+1}}{\alpha+1} \sum_{k=1}^6 A_k^u q_k^u (C_k^u)^{\alpha+1} \quad (A.3.38)$$

$$*W^u = \frac{r^{\alpha+1}}{\alpha+1} \sum_{k=1}^6 A_k^u r_k^u (C_k^u)^{\alpha+1}$$

where

$$\begin{aligned} p_k^u &= B_{11}^u (\mu_k^u)^2 + B_{12}^u - B_{16}^u \mu_k^u + \lambda_k^u (B_{15}^u \mu_k^u - B_{14}^u) \\ q_k^u &= B_{12}^u \mu_k^u + \frac{B_{22}^u}{\mu_k^u} - B_{26}^u + \lambda_k^u (B_{25}^u - \frac{B_{24}^u}{\mu_k^u}) \\ r_k^u &= B_{14}^u \mu_k^u + \frac{B_{24}^u}{\mu_k^u} - B_{46}^u + \lambda_k^u (B_{45}^u - \frac{B_{44}^u}{\mu_k^u}) \end{aligned} \quad (A.3.39)$$

Similar expressions hold for the lower layer with coefficients A_k^{ℓ} .

From the bonding conditions along $\theta = 0^\circ$,

$$\sum_{k=1}^6 A_k^u \mu_k^u = \sum_{k=1}^6 A_k^{\ell} \mu_k^{\ell}$$

$$\sum_{k=1}^6 A_k^u = \sum_{k=1}^6 A_k^{\ell}$$

$$\sum_{k=1}^6 A_k^u \lambda_k^u = \sum_{k=1}^6 A_k^{\ell} \lambda_k^{\ell}$$

(cont'd)

$$\sum_{k=1}^6 A_k^u p_k^u = \sum_{k=1}^6 A_k^l p_k^l$$

$$\sum_{k=1}^6 A_k^u q_k^u = \sum_{k=1}^6 A_k^l q_k^l \quad (A.3.40)$$

$$\sum_{k=1}^6 A_k^u r_k^u = \sum_{k=1}^6 A_k^l r_k^l$$

The above six equations provide a relationship between A_k^u and A_k^l .

From the stress-free conditions at $\theta = \frac{\pi}{2}$

$$\sum_{k=1}^6 A_k^u (\mu_k^u)^{2+\alpha} = 0$$

$$\sum_{k=1}^6 A_k^u (\mu_k^u)^{1+\alpha} = 0 \quad (A.3.41)$$

$$\sum_{k=1}^6 A_k^u \lambda_k^u (\mu_k^u)^{1+\alpha} = 0$$

and also from the stress-free conditions at $\theta = -\frac{\pi}{2}$

$$\sum_{k=1}^6 A_k^l (-\mu_k^l)^{2+\alpha} = 0$$

$$\sum_{k=1}^6 A_k^l (-\mu_k^l)^{1+\alpha} = 0 \quad (\text{cont'd})$$

$$\sum_{k=1}^6 A_k^{\ell} \lambda_k^{\ell} (-\mu_k^{\ell})^{1+\alpha} = 0 \quad (\text{A.3.42})$$

Combining eqs. (A.3.40), (A.3.41) and (A.3.42), we obtain a system of homogeneous equations

$$\underline{C}(\alpha) \underline{A}^u = 0 \quad (\text{A.3.43})$$

where

$$\underline{A}^u = \begin{Bmatrix} A_1^u \\ \vdots \\ A_6^u \end{Bmatrix} \quad (\text{A.3.44})$$

and $\underline{C}(\alpha)$ is a 6×6 matrix with eigenvalue α . For the material properties used in this study and $\pm 45^\circ$ layer, the first eigenvalue corresponding to stress singularity is $\alpha = -0.0255756$.

Using eigenvalues and the corresponding eigenvectors, we may construct the assumed stress and displacement fields. For example, for assumed stress $*\sigma_{xx}^u$,

$$*\sigma_{xx}^u = \sum_{i=1}^n \text{Re} [r^{\alpha_i} \sum_{k=1}^6 (A_k^u)_{\alpha=\alpha_i} S_k^u (C_k^u)^{\alpha_i}] \beta_i \quad (\text{A.3.45})$$

with

$$S_k^u = (\mu_k^u)^2$$

The other assumed stress components have a similar expression with proper definition of S_k^u as follows:

<u>Stress Components</u>	$\frac{S_k^u}{k}$
$*\sigma_{yy}^u$	1.0
$*\sigma_{xy}^u$	$-\mu_k^u$
$*\sigma_{xz}^u$	$\lambda_k^u \mu_k^u$
$*\sigma_{yz}^u$	$-\lambda_k^u$

For assumed displacement $*U^u$,

$$*U^u = \sum_{i=1}^n \operatorname{Re} \left[\frac{r^{\alpha_i+1}}{\alpha_i+1} \sum_{k=1}^6 (A_k^u)_{\alpha=\alpha_i} p_k^u (C_k^u)^{\alpha_i+1} \right] \beta_i \quad (\text{A.3.46})$$

The expression for $*V^u$ is obtained by replacing p_k^u in eq. (A.3.46) with q_k^u . Likewise, the expression for $*W^u$ is obtained by replacing p_k^u with r_k^u . Similar expressions hold for $\sigma_{xx}^l \dots \sigma_{xy}^l$, $*U^l$, $*V^l$ and $*W^l$ for the lower layer. The coefficients $\beta_1, \beta_2 \dots$ are unknown free parameters. In the present study a four term approximation ($n=4$) was used.